2022 International Symposium on Nonlinear Theory and Its Applications,
NOLTA2022, Virtual, December 12-15, 2022

Tunable Period-One Dynamical Millimeter-Wave Generation by Cascaded Injection of Lasers

Luan Zhang[1] and Sze-Chun Chan[1,2,*]

[1] Department of Electrical Engineering, City University of Hong Kong, Hong Kong, China
[2] State Key Laboratory of Terahertz and Millimeter Waves, City University of Hong Kong, Hong Kong, China
*Email: scchan@cityu.edu.hk

Abstract– For generating tunable photonic millimeter-wave (mm-wave) signals, the period-one (P1) nonlinear dynamics of semiconductor lasers are investigated through cascaded optical injection. Starting from a continuous-wave master laser, a primary slave laser is optically injected into P1 dynamics at a microwave frequency f_0. It in turn injects a secondary slave laser that enhances the harmonic component of the intensity oscillation at $2f_0$, which is typically in the mm-wave band. By applying on the injection a subharmonic modulation at $f_0/3$, the frequency fluctuation of the harmonic component is stabilized. By adjusting the operating conditions of lasers, the wide frequency tunability of P1 dynamics enables the continuous tuning of $2f_0$. Experimentally, tunable photonic mm-wave generation of $2f_0$ is demonstrated to up to 42 GHz with a range of over 5 GHz, while the electrical linewidth is always below the measurement resolution bandwidth of 1 kHz through the subharmonic modulation.

1. Introduction

Photonic microwave generation has long been investigated for various applications such as radio-over-fiber communications, arbitrary waveform generation, signal processing, and ranging. Generation of ultra-wideband signals, manipulation of high-frequency signals, and transmission of microwave signals over low-loss optical fibers are allowed by photonic techniques. Although these are difficult to be achieved by traditional electronic methods [1, 2], different approaches have been developed for photonic microwave generation over the last two decades, including the use of optoelectronic oscillators, mode-locked lasers, dual-wavelength lasers, and so on [3-6]. In recent years, nonlinear dynamics of semiconductor lasers have been investigated for many applications such as modulation bandwidth enhancement, random number generation, secure communications, and square-wave generation [7-9]. The period-one (P1) nonlinear dynamics of optically injected semiconductor lasers are particularly attractive for photonic microwave generation [10-19], where the limit-cycle behaviors are utilized [20, 21]. The P1 dynamics are advantageous in photonic microwave generation due to wide continuous frequency tunability, large intensity modulation depth, and simple optical control [18, 19]. A semiconductor laser in P1 dynamics emits with a periodically oscillatory intensity at a microwave frequency f_0, which can be tuned to more than 100 GHz even when the relaxation resonance frequency of the laser is merely about 10 GHz [15, 17]. To suppress the phase noise of the P1 dynamics, optical feedback and optoelectronic feedback were investigated [10, 14, 15]. In addition, subharmonic locking was utilized to suppress the phase noise associated with the P1 dynamics through various forms of modulations, which were achieved through direct modulation of the bias current or external electro-optic modulators [13, 16-19, 22]. However, most of these approaches were limited to the fundamental P1 frequency f_0 of a single optically injected laser [13-19].

In this work, cascaded injection is experimentally investigated for tunable millimeter-wave (mm-wave) generation by enhancing the harmonics of the P1 dynamics using two slave lasers. P1 dynamics at a fundamental microwave frequency f_0 is first induced by a continuous-wave (CW) injection in a primary slave laser SL_1, which is then used to inject a secondary slave laser SL_2 for enhancing the harmonic component of P1 dynamics at $2f_0$. As a result, photonic mm-wave generation at $2f_0$ = 42 GHz is achieved based on the fundamental P1 frequency at f_0 = 21 GHz. Subharmonic locking by an external modulation at $f_0/3$ is applied to stabilize the frequency fluctuation of the generated mm-wave signal at $2f_0$, leading to a reduced electrical linewidth of less than the measurement resolution bandwidth of 1 kHz. While the approach has been studied up to 72 GHz using specific mm-wave measurements [18], the tunability is demonstrated here for the frequency $2f_0$ from 42 GHz to 37 GHz in covering a 5-GHz range. This is realized by carefully adjusting the operating conditions of the slave lasers. By adding more slave lasers, cascaded injection can be extended for mm-wave generation at higher frequencies.

2. Experimental Setup

Figure 1 shows the experimental setup of the cascaded injection using semiconductor lasers for tunable P1 dynamical mm-wave generation. Two slave lasers SL_1 and SL_2 are 1.55-μm single-mode distributed-feedback lasers (Apico CMP-LD-1550-BTF), which have thresholds of about 10 mA when temperature-stabilized at around 20 ºC. A CW optical injection is provided by a similar laser at optical frequency ν_0 = 193.5 THz via an optical amplifier. To begin with, the injection is split by a fiber coupler FC_1 and sent through a 10-GHz electro-optic phase modulator MOD (Thorlabs LN65S-FC), a polarization controller PC_1, and a circulator for injection into SL_1. Then, the emission of SL_1 is injected into SL_2 through a polarization controller PC_2 and a circulator. As a result of the cascaded injection, SL_2 emits at position Q_c. The polarizations of injections into SL_1 and SL_2 are matched by optimizing PC_1 and PC_2. The output mm-wave signal at position Q_s is obtained by summing the emission from SL_2 and CW light at ν_0. For monitoring, an optical spectrum analyzer (YOKOGAWA AQ6370) with a resolution of 2.5 GHz is used. The corresponding electrical signals are detected by a 70-GHz photodetector (Finisar XPDV3120) and measured by a 43-GHz electrical spectrum analyzer (Advantest U3772) after the light is amplified by a fiber amplifier to maintain a constant average optical power in measurements.

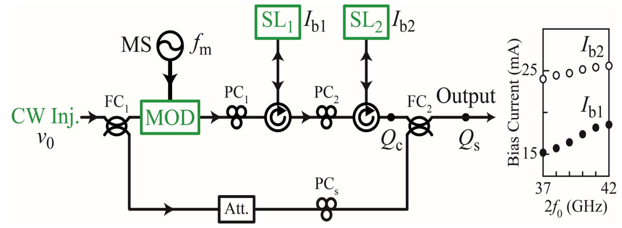

Figure 1 Schematic of cascaded injection of semiconductor lasers for tunable P1 dynamical mm-wave generation. CW Inj., continuous-wave optical injection; SL_1, primary slave laser; SL_2, secondary slave laser; MS, microwave source; MOD, electro-optic modulator; FC, fiber coupler; PC, polarization controller; Att., attenuation [18]. Inset: bias currents of SL_1 (closed circles) and SL_2 (open circles) as a function of the generated mm-wave frequency $2f_0$.

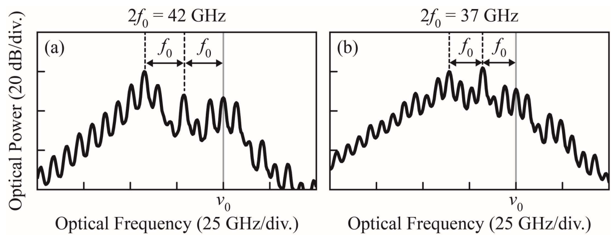

Figure 2 Optical spectra of the emissions from SL_2 at Q_c for mm-wave generation at $2f_0$ = (a) 42 GHz and (b) 37 GHz. MOD is switched on at frequency $f_m = f_0/3$.

3. Experimental Results

For mm-wave generation at $2f_0$ = 42 GHz, P1 dynamics at a fundamental frequency f_0 of 21 GHz is first invoked by the injection in SL_1, which is biased at I_{b1} = 17 mA and emits about 1.4 mW via the fiber-pigtail. Though SL_1 emits at around 12 GHz below ν_0 when free-running, it exhibits the P1 dynamics at f_0 = 21 GHz because of the injection with a power at the pigtail of about 0.8 mW. The fundamental P1 frequency f_0 = 21 GHz is higher than the relaxation resonance frequencies of both slave lasers, which are less than 10 GHz. The emission of SL_1 contains a strong regenerative component at ν_0 with several other components equally separated by f_0, as generated by the P1 dynamics. The cavity resonance of SL_1 is redshifted and amplifies the P1 component at $\nu_0 - f_0$, as attributed to the antiguidance effect [11]. The P1 component at $\nu_0 - f_0$ is nearly as strong as the regeneration at ν_0 [18]. As for mm-wave generation at $2f_0$, SL_1 emits merely a relatively weak P1 harmonic component at $\nu_0 - 2f_0$ [11, 15, 18]. To enhance the harmonic of the P1 dynamics, the emission from SL_1 is in turn injected into SL_2, which is biased at I_{b2} = 25 mA and emits about 3.4 mW via the fiber-pigtail when free-running. Although SL_2 has a free-running optical frequency of about 40 GHz below ν_0, it is injection-locked by SL_1 into emitting ν_0 along with the components equally separated by f_0 = 21 GHz. The emission of SL_2 inherits the two components at ν_0 and $\nu_0 - f_0$, while emitting the strongest component at $\nu_0 - 2f_0$ due to enhancement by its redshifted cavity resonance [18]. Therefore, photonic mm-wave generation at $2f_0$ = 42 GHz is enabled when the optical components at ν_0 and $\nu_0 - 2f_0$ beat. Because of the intrinsic noise of the lasers, the generated mm-wave signal at $2f_0$ = 42 GHz has a relatively broad linewidth on the order of 10 MHz.

To suppress the phase noise of the generated mm-wave at $2f_0$ = 42 GHz, the CW injection is modulated by switching on a stable microwave source MS that is connected to the modulator MOD. The driving signal is sinusoidal at a modulation frequency f_m of $f_0/3$ = 7 GHz with a power of 16 dBm from MS. Subharmonic locking is achieved through MOD by a phase modulation that has a depth of about 0.9 (rad). The emission of SL_2 now has P1 components coinciding with every three sidebands of the phase modulation, as shown in Fig. 2(a). For example, the P1 harmonic component at $\nu_0 - 2f_0$ coincides with the modulation sideband at $\nu_0 - 6f_m$, which is much strengthened by the cascaded injection [18]. The corresponding power spectrum is recorded in Fig. 3(a), where the electrical linewidth of the generated mm-wave signal at $2f_0$ = 42 GHz is drastically reduced to the less than the measurement resolution bandwidth of 1 kHz. The linewidth reduction by more than three orders of magnitude indicates an effective stabilization of frequency fluctuation for mm-wave generation at $2f_0$.

Most importantly, the frequency tunability of mm-wave generation at $2f_0$ is demonstrated over 5 GHz between 42 GHz and 37 GHz by varying the bias currents I_{b1} and I_{b2}, as recorded by the inset in Fig. 1, while keeping the injection power and frequency unchanged. The modulation frequency at $f_m = f_0/3$ is accordingly adjusted when $2f_0$ is tuned from 42 GHz to 37 GHz in order to maintain subharmonic locking. Figures 2(a) and 2(b) respectively show the optical spectra of emissions from SL_2 at Q_c when $2f_0$ is 42 GHz and 37 GHz. In Fig. 3, the power spectra measured at Q_c for the emissions of SL_2 are recorded by setting the span to 100 kHz and the center frequency to $2f_0$, which is tuned from 42 GHz to 37 GHz with a step of 1 GHz. Throughout Fig. 3, the recorded linewidths are limited by the measurement equipment to 1 kHz, although it is known that a linewidth of less than 50 Hz was experimentally demonstrated at 72 GHz based on a high-frequency electrical spectrum analyzer when applying subharmonic locking at $f_m = f_0/4$ = 9 GHz [18].

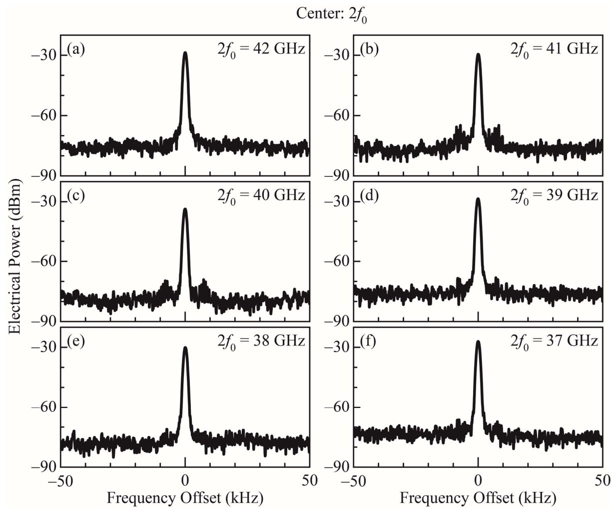

Figure 3 Power spectra of the emissions from SL_2 at Q_c for mm-wave generation at $2f_0$ = (a) 42 GHz, (b) 41 GHz, (c) 40 GHz, (d) 39 GHz, (e) 38 GHz, and (f) 37 GHz. MOD is switched on at $f_m = f_0/3$. The horizontal axes of the power spectra are offset to center frequencies at different $2f_0$. Resolution bandwidth: 1 kHz.

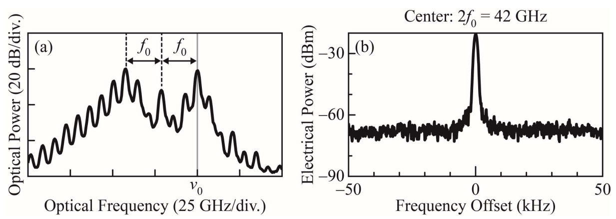

Figure 4 (a) Optical spectrum and (b) power spectrum measured at Q_s with coherent addition of the CW injection for the mm-wave output at $2f_0$ = 42 GHz. MOD is switched on at f_m = 7 GHz. The horizontal axis of the power spectrum is offset to $2f_0$.

To enhance the intensity modulation depth of the generated photonic mm-wave signal at $2f_0$, coherent addition is applied at position Q_s in Fig. 1 by summing up the emission from SL_2 and CW injection light, which propagates through two 3-dB fiber couplers FC_1 and FC_2, an attenuator, and a controller PC_s for polarization matching. Figure 4 shows the optical spectrum and power spectrum measured at Q_s for mm-wave output at $2f_0$ = 42 GHz. The optical components at v_0 and $v_0 - 2f_0$ become nearly equally strong, as shown in Fig. 4(a), implying that the intensity modulation depth is increased. While the narrow electrical linewidth is maintained, the mm-wave output at $2f_0$ = 42 GHz is strengthened by the coherent addition in Fig. 4(b), as compared with Fig. 3(a). The optical path lengths of the upper and lower arms in Fig. 1 between FC_1 and FC_2 are matched to within 0.1 m that is orders of magnitude shorter than the coherence length of the CW injection light [18].

4. Discussion

The single-sideband (SSB) phase noise is measured to demonstrate the stability of the 42-GHz mm-wave output at position Q_s. The SSB phase noise is obtained by normalizing the power spectrum to its peak [13, 18, 22]. As the black curve in Fig. 5(a) shows, the SSB phase noise spectrum of the 42-GHz mm-wave output is lower than –75 dBc/Hz at an offset of 10-kHz, which is limited by the electrical spectrum analyzer. For reference, the SSB phase noise spectrum of the driving signal at f_m = 7 GHz is directly measured for the source MS, as the gray curve in Fig. 5(a) shows. Ideally, perfect subharmonic locking yields a phase noise identical to that of the source MS with an offset by $+20 \log_{10}(2f_0/f_m)$ = 15.6 dB [13, 22]. Contrasting the ideal locking, the excess noise of the 42-GHz mm-wave output is plotted in Fig. 5(b) by subtracting $20 \log_{10}(2f_0/f_m)$ from the gap between the two curves in Fig. 5(a). The excess noise is essentially between 0 dB and 10 dB in the range of frequency offsets measured.

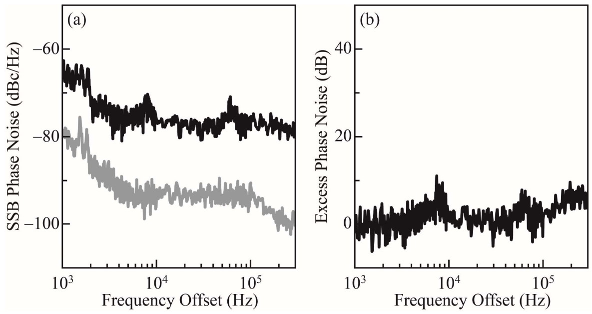

Figure 5 (a) SSB phase noise of the 42-GHz output at Q_s (black) and of MS (gray). (b) Excess phase noise of the output as compared to ideal locking.

5. Conclusion

In conclusion, cascaded injection of semiconductor lasers is investigated to enhance the P1 dynamics harmonics for tunable mm-wave generation. The CW optical injection induces SL_1 into P1 dynamics at a fundamental frequency f_0. SL_1 in turn injects SL_2 for enhancement of the P1 harmonic component at $2f_0$. Tunable photonic mm-wave generation at $2f_0$ is obtained, as demonstrated over a range of 5 GHz up to 42 GHz. Meanwhile, subharmonic locking is applied for noise suppression. Coherent addition is also used to strengthen the mm-wave signal generated at $2f_0$. Such a tunable cascaded injection can possibly be extended for photonic mm-wave generation at higher frequencies using more slave lasers.

Acknowledgments

The work described in this work was fully supported by the Research Grants Council of Hong Kong, China (CityU 11200618 and T42-103/16-N).

References

[1] J. Capmany and D. Novak, "Microwave photonics combines two worlds," *Nat. Photonics*, vol. 1, pp. 319-330, 2007.

[2] D. Marpaung, J. Yao, and J. Capmany, "Integrated microwave photonics," *Nat. Photonics*, vol. 13, pp. 80-90, 2019.

[3] X. S. Yao and L. Maleki, "Multiloop optoelectronic oscillator," *IEEE J. Quantum Electron.*, vol. 36, pp. 79-84, 2000.

[4] W. Zhang and J. Yao, "Silicon photonic integrated optoelectronic oscillator for frequency-tunable microwave generation," *J. Lightwave Technol.*, vol. 36, pp. 4655-4663, 2018.

[5] C. Y. Lin, F. Grillot, Y. Li, R. Raghunathan, and L. F. Lester, "Microwave characterization and stabilization of timing jitter in a quantum-dot passively mode-locked laser via external optical feedback," *IEEE J. Sel. Top. Quantum Electron.*, vol. 17, pp. 1311-1317, 2011.

[6] M. Rahim, K. Zeb, Z. Lu, G. Pakulski, J. Liu, P. Poole, C. Song, P. Barrios, W. Jiang, and X. Zhang, "Monolithic InAs/InP quantum dash dual-wavelength DFB laser with ultra-low noise common cavity modes for millimeter-wave applications," *Opt. Express*, vol. 27, pp. 35368-35375, 2019.

[7] Z. Liu and R. Slavik, "Optical injection locking: from principle to applications," *J. Lightwave Technol.*, vol. 38, pp. 43-59, 2020.

[8] M. Sciamanna and K. A. Shore, "Physics and applications of laser diode chaos," *Nat. Photonics*, vol. 9, pp. 151-162, 2015.

[9] J. X. Dong, J. Ruan, L. Zhang, J. P. Zhuang, and S. C. Chan, "Stable-unstable switching dynamics in semiconductor lasers with external cavities," *Phys. Rev. A*, vol. 103, p. 053524, 2021.

[10] S. C. Chan and J. M. Liu, "Tunable narrow-linewidth photonic microwave generation using semiconductor laser dynamics," *IEEE J. Sel. Top. Quantum Electron.*, vol. 10, pp. 1025-1032, 2004.

[11] S. C. Chan, "Analysis of an optically injected semiconductor laser for microwave generation," *IEEE J. Quantum Electron.*, vol. 46, pp. 421-428, 2010.

[12] A. Hurtado, J. Mee, M. Nami, I. D. Henning, M. J. Adams, and L. F. Lester, "Tunable microwave signal generator with an optically-injected 1310 nm QD-DFB laser," *Opt. Express*, vol. 21, pp. 10772-10778, 2013.

[13] Y. H. Hung and S. K. Hwang, "Photonic microwave stabilization for period-one nonlinear dynamics of semiconductor lasers using optical modulation sideband injection locking," *Opt. Express*, vol. 23, pp. 6520-6532, 2015.

[14] J. P. Zhuang and S. C. Chan, "Tunable photonic microwave generation using optically injected semiconductor laser dynamics with optical feedback stabilization," *Opt. Lett.*, vol. 38, pp. 344-346, 2013.

[15] J. P. Zhuang and S. C. Chan, "Phase noise characteristics of microwave signals generated by semiconductor laser dynamics," *Opt. Express*, vol. 23, pp. 2777-2797, 2015.

[16] L. Fan, G. Q. Xia, J. J. Chen, X. Tang, Q. Liang, and Z. M. Wu, "High-purity 60 GHz band millimeter-wave generation based on optically injected semiconductor laser under subharmonic microwave modulation," *Opt. Express*, vol. 24, pp. 18252-18265, 2016.

[17] C. H. Tseng, C. T. Lin, and S. K. Hwang, "V- and W-band microwave generation and modulation using semiconductor lasers at period-one nonlinear dynamics," *Opt. Lett.*, vol. 45, pp. 6819-6822, 2020.

[18] L. Zhang and S. C. Chan, "Cascaded injection of semiconductor lasers in period-one oscillations for millimeter-wave generation," *Opt. Lett.*, vol. 44, pp. 4905-4908, 2019.

[19] L. Zhang and S. C. Chan, "Perturbing period-one laser dynamics for frequency-modulated microwave generation with external locking," *Opt. Lett.*, vol. 47, pp. 4483-4486, 2022.

[20] T. B. Simpson, J. M. Liu, M. AlMulla, N. G. Usechak, and V. Kovanis, "Limit-cycle dynamics with reduced sensitivity to perturbations," *Phys. Rev. Lett.*, vol. 112, p. 023901, 2014.

[21] A. Karsaklian Dal Bosco, K. Kanno, A. Uchida, M. Sciamanna, T. Harayama, and K. Yoshimura, "Cycles of self-pulsations in a photonic integrated circuit," *Phys. Rev. E*, vol. 92, p. 062905, 2015.

[22] G. J. Schneider, J. A. Murakowski, C. A. Schuetz, S. Shi, and D. W. Prather, "Radiofrequency signal-generation system with over seven octaves of continuous tuning," *Nat. Photonics*, vol. 7, pp. 118-122, 2013.